

1 **Inflammasome targeting with an NLRP3 agonist therapy is feasible but**
2 **ineffective in murine hepatocellular carcinoma models with liver damage**

3 Zhangya Pu^{1,2,3}, Zelong Liu¹, Jiang Chen¹, Koetsu Inoue¹, Zhiping Ruan¹, Lingling Zhu¹, Hiroto
4 Kikuchi¹, Aya Matsui¹, Peigen Huang¹, Dan G. Duda^{1,*}

5 **1** Edwin L. Steele Laboratories for Tumor Biology, Department of Radiation Oncology,
6 Massachusetts General Hospital, MA, USA, **2** Department of Infectious Diseases, Hunan Key
7 Laboratory of Viral Hepatitis, Xiangya Hospital, Central South University, Changsha, Hunan
8 Province, 410008, China, **3** Department of Infectious Disease, The First Affiliated Hospital,
9 Zhejiang University, Zhanghou, Zhejiang, 310006, China.

10 **Short Title: NLRP3 targeting is not active against murine HCC**

11 ***Address correspondence to:** Dan G. Duda, DMD, PhD, Massachusetts General Hospital, CNY-
12 3.407, 13th Street, Charlestown, MA, USA, 02129; phone: (617) 726-4648; fax: (617) 726-1962;
13 email: duda@steele.mgh.harvard.edu

14 **Abstract**

15 Co-inhibition of programmed cell death receptor-1 (PD-1) and vascular endothelial growth
16 factor receptor (VEGFR) pathway has shown efficacy in hepatocellular carcinoma (HCC). NLRP3
17 is a component of the inflammasome involved in the initiation, development, and progression of
18 multiple cancers. We examined whether adding an NLRP3 agonist to dual PD-1/VEGFR inhibitors
19 is feasible and can address treatment resistance in orthotopic HCC in mice with underlying liver
20 damage. Mice with established tumors were treated with an NLRP3 agonist alone, combination of
21 anti-VEGFR2 or the multikinase inhibitor regorafenib with anti-PD1 antibodies, or their
22 combination. In all models tested, NLRP3 agonist therapy showed acceptable toxicity but no effect
23 on tumor growth delay, disease morbidity, or survival. Pharmacodynamic analyses confirmed the
24 effects of NLRP3 agonist therapy on inflammasome, evidenced by a significant elevation in
25 plasma levels of pro-inflammatory cytokines such as IL-1 β . However, these changes were not
26 detectable in tumor tissues, where we detected increased expression of immunosuppressive
27 markers IL-6, KC/GRO, CCL9, and IL-18, and immune checkpoint molecules (PD1, PD-L1, and
28 CTLA-4) after NLRP3 agonist therapy. Thus, modulation of the inflammasome with a novel
29 NLRP3 agonist was feasible in mice with orthotopic HCC and liver damage but did not enhance
30 efficacy when combined with anti-PD1/VEGFR therapies.

31 **Keywords:** Hepatocellular carcinoma; NLRP3 agonist; Programmed death receptor 1 (PD1);
32 Vascular endothelial growth factor receptor (VEGFR); liver damage.

33 **Introduction**

34 Hepatocellular carcinoma (HCC) is the most prevalent malignancy of the liver. It is currently
35 ranked a leading cause of cancer-related mortality worldwide and over 850,000 patients are
36 diagnosed with HCC every year [1, 2]. HCC is an aggressive disease occurring predominantly in
37 patients with chronic liver damage caused by viral infections (hepatitis B and C virus), excessive
38 alcohol intake, exposure to aflatoxin, non-alcoholic steatohepatitis (NASH), or metabolic
39 disorders. These factors result in a hepatic environment dominated by inflammation, which
40 increases the risk of carcinogenesis and facilitates the progression of HCCs [3, 4].

41 In the context of HCC, the presence of a significant immune cell infiltration (referred to as the
42 “immunologically hot” tumor) is generally correlated with a better prognosis, attributed to a
43 greater degree of pre-existing anti-tumor immunity [5, 6]. However, the tumor microenvironment
44 of HCC is usually characterized by immunosuppression, mediated by multiple cellular and
45 biochemical factors involved in immune evasion mechanisms during HCC progression [7, 8].
46 These mechanisms include the up-regulation of immune checkpoint molecules on HCC and
47 stromal cells promoting the exhaustion of effector immune cells (CD4⁺ and CD8⁺ T lymphocytes),
48 increased infiltration of immunosuppressive cells [tumor-associated macrophages (TAM), T
49 regulatory cells (Tregs), and myeloid-derived suppressor cells (MDSCs)], increased expression of
50 inflammatory cytokines such as IL-6; and the dysfunction of the antigen-presenting process [9-
51 12].

52 Development of immunotherapy approaches to activate anti-tumor immunity in HCC has
53 seen substantial progress in the last few years with the advent of immune checkpoint blockade
54 (ICB) targeting the programmed cell death receptor 1 (PD-1)/PD ligand 1 (PD-L1) pathway.
55 Monotherapy with anti-PD-1 antibodies (nivolumab, pembrolizumab) was approved by the US

56 FDA based on phase I/II trials in patients with advanced HCC because of the promising objective
57 response rate but especially due to durable disease control and favorable safety profiles [13] [14].
58 This pattern of response contrasted to that seen after antiangiogenic therapies, which increased
59 overall survival (OS) but whose benefits were more transient in advanced HCC [15, 16].
60 Randomized phase III trials of nivolumab and pembrolizumab monotherapy did not reach the
61 prespecified endpoints of survival benefit [17, 18], but a more recent phase III trial of
62 pembrolizumab met the primary endpoint of OS in Asian patients with advanced HCC previously
63 treated with sorafenib (News release. Merck. September 27, 2021. Accessed September 28, 2021).

64 To enhance the limited efficacy of anti-PD-1 therapy alone, several combinatorial strategies
65 have been developed, including ICB combinations or ICBs with antiangiogenic drugs [8, 19]. We
66 have previously shown that anti-PD-1 antibodies with anti-VEGFR therapies (antibodies or kinase
67 inhibitors) can be effective in murine HCC models, in part by normalizing the abnormal tumor
68 vessels, decreasing the infiltration of Tregs and MDSCs, and enhancing the infiltration and
69 activation of effector CD8 T cells [20] [21]. Recently, a phase III clinical trial (IMbrave150) of
70 combined atezolizumab (an anti-PD-L1 antibody) and bevacizumab (an anti-VEGF antibody) was
71 the first regimen to prolong OS compared to standard antiangiogenic tyrosine kinase treatment
72 with sorafenib [22]. Multiple combinatorial approaches are currently ongoing aiming to establish
73 the efficacy of antiangiogenic tyrosine kinase drugs with anti-PD-1/PD-L1 treatment [19, 23] Yet,
74 despite these significant and exciting new developments, the majority of HCC patients show
75 resistance to these ICB-based approaches, and addressing this unmet need will require new
76 approaches to combat immunosuppression [23].

77 Inflammation due to liver damage modulates the initiation, development, and progression of
78 carcinogenesis, and involves innate and adaptive immune responses mediated by infiltrating cells

79 such as MDSCs, tumor-associated macrophages (TAMs), or lymphocyte subsets [8, 24, 25]. The
80 inflammatory reaction is mediated by specific cytoplasmic multimetric protein complexes called
81 inflammasomes [26]. Inflammasomes include three key domains of the nucleotide-binding domain
82 (NBD), oligomerization domain (NOD)-like receptors (NLRs), and absent in melanoma 2 (AIM2)
83 and belong to a large family of pattern recognition receptors (PRRs). The PRRs are associated
84 with recognition of pathogen-/ danger-associated molecular patterns (PAMPs and DAMPs) and
85 lead to the activation, maturation, and up-regulation of pro-inflammatory cytokines of IL-1 β and
86 IL-18 [27].

87 Among inflammasome components, the nod-like receptor protein 3 (NLRP3) plays important
88 role in several types of autoimmune and inflammatory diseases such as cold-induced
89 autoinflammatory syndrome (CAPS). Moreover, several recent studies reported that mutation or
90 copy number alteration of the NLRP3 gene was associated with oncogene activation [26, 27]. The
91 function of NLRP3 inflammasome in tumor progression or anti-tumor immunity remains unclear.
92 Constitutive activation of the NLRP3 inflammasome was correlated to the malignant phenotype
93 of human melanoma, lung cancer, and colon carcinoma [27, 28]. Conversely, Wei et al. reported
94 that the expression of all NLRP3 components is either lost or downregulated in the tumor tissues
95 than in the corresponding adjacent non-tumor tissues in HCC [29]. In addition, targeting NLRP3
96 inflammasome using pharmacological agents may hinder the proliferative and metastatic ability
97 of HCC [29, 30]. Moreover, the specific role of NLRP3 targeting in ICB and antiangiogenic
98 treatment-resistance in HCC is unknown. Here, we examined the feasibility and efficacy of a new
99 NLRP3 agonist alone or with dual anti-PD-1/VEGFR agents in murine HCC models with
100 underlying liver damage.

101 **Materials and Methods**

102 **Cells and culture condition**

103 Two murine HCC lines were used in the current study: HCA-1 cells, established in the Steele
104 Laboratories on the C3H mouse background [31, 32], and RIL-175 cells, a *p53*-null/*Hras*-mutant
105 line syngeneic to C57Bl/6 mouse background (a kind gift from Dr. Tim Greten, NCI, Bethesda,
106 USA). Cells were cultured in Dulbecco's Modified Eagle's Medium (DMEM) (ThermoFisher,
107 USA) was supplemented with 10% fetal bovine serum (FBS) (Hyclone, SH30071.03) and
108 penicillin-streptomycin at a concentration of 100U/ml and 100µg/ml, respectively, at 37°C with 5%
109 CO₂. Cells were routinely examined for mycoplasma contamination and authenticated before *in*
110 *vivo* experiments.

111 **Orthotopic HCC model**

112 The orthotopic HCC model with liver damage is described in detail elsewhere [33]. Briefly, to
113 induce chronic liver damage, mice were treated three times a week with carbon tetrachloride (CCl₄)
114 (Sigma Aldrich, Saint Louis, MO) via oral gavage for 8-12 weeks. One million murine HCC cells
115 in Matrigel (Mediatech/Corning, Manassas, VA) in 1:1 solution were implanted in syngeneic mice
116 (HCA-1 cells in C3H mice and RIL-175 in C57Bl/6). Tumor initiation and growth were monitored
117 using high-frequency ultrasonography twice a week. Mice with established HCC were randomized
118 to the treatment groups when the diameter of the tumor reached approximately 5mm. Per protocol,
119 the experimental endpoint for efficacy studies was moribund status, defined as the following
120 symptoms: significant distress, weight loss of more than 15% compared to pretreatment, body
121 status score >2, and diameter of primary tumor of more 15 mm. All animal experiments were
122 conducted using a protocol approved by the Institutional Animal Care and Use Committee of the
123 Massachusetts General Hospital, Boston, MA.

124 **Reagents and Treatments**

125 The NLRP3 agonist (BMT-392959) and anti-mouse PD-1 antibody (isotype-matched
126 IgG1:D265A) were all provided by Bristol Myers Squibb Company (USA). These agents were
127 administered as per the manufacturer's recommendations: NLRP3 agonist was given by
128 intraperitoneal injection (i.p.) at a dose of 10mg/kg once a week, and anti-mouse PD-1 antibody
129 or IgG1 control was administrated at a dose of 10mg/kg via i.p. injections every 4 days. Anti-
130 mouse VEGFR2 antibody (DC101) was purchased from BioXcell (Lebanon, USA) and was given
131 i.p. at a dose of 20 mg/kg three times a week, as described [20]. The multitargeted kinase inhibitor
132 regorafenib was purchased from Selleck Chemicals and administrated at a dose of 10 mg/kg
133 [dissolved in 34% 1,2-propandiol and 34% PEG400 (SigmaAldrich), 12 % pluronic F68 (Thermo
134 Fischer, MA, USA), and 20% purified water] by daily oral gavage, as described [21].

135 **Proteomic and transcriptomic analyses in time-matched studies in vivo**

136 Blood and tumor samples were collected in separate time-matched experiments using the
137 orthotopic HCC model in C57Bl/6 mice. Tissue collection was performed after 4-hr and 24-hr
138 after treatment with one dose of NLRP3 agonist (10mg/kg) or control in mice with established
139 orthotopic murine RIL-175 HCCs.

140 To study protein levels of cytokines and chemokines, we separated plasma from the blood
141 samples and extracted proteins from the tissue samples. Briefly, whole blood samples were
142 collected in anticoagulant (EDTA)-coated tubes and processed for plasma separation by
143 centrifugation at 4°C. For protein extraction, each tumor tissue sample was placed in 500 µl/sample
144 lysis buffer. The samples were ground, and then centrifugated at 4°C to collect the liquid phase for
145 protein concentration measurements.

146 Measurements were performed in duplicate for plasma samples and triplicate for tumor tissue
147 samples using multiplexed array kits from Meso Scale Discovery (Gaithersburg, MD, USA):
148 proinflammatory panel I mouse kit (catalog: K15048D), which includes interferon (IFN)- γ ,
149 interleukin (IL)-1 β , IL-2, IL-4, IL-5, IL-6, IL-10, IL12p70, TNF- α , and KC/GRO, and Cytokine
150 panel I mouse kit (catalog: K15245D), which includes CCL2, CCL3, CXCL-2, CXCL-10, IL-
151 27p28, IL-9, and IL-33. The procedure was performed as per the manufacturer's protocols, and
152 plates were analyzed using electrochemiluminescence-based detection on an SQ120 machine.

153 In addition, total RNA was extracted from the tumor tissue samples using an RNeasy Mini Kit
154 (Qiagen Inc.), and the quality and concentration were analyzed using a NanoDrop
155 Spectrophotometer. Complementary DNA was synthesized using the reverse transcription kit
156 (PrimeScript RT reagent Kit) and quantitative (q)PCR was performed using iTaq Universal SYBR
157 Green Supermix (Bio-Rad Laboratories, Hercules, CA). The housekeeping gene GAPDH was used
158 for reference. The primers used in this study for qPCR are listed in **Table S1**. The relative
159 amplified amount of mRNA was calculated by the $2^{-\Delta\Delta CT}$ method.

160 **Statistical analysis**

161 Continuous variables were compared using Student's t-test with one-tail. When the experiments
162 included more than two groups, the one-way ANOVA with a Brown-Forsythe test was used for
163 multiple comparisons. Categorical variables were analyzed using χ^2 (Chi-squared) or Fisher's test.
164 Kaplan-Meier (K-M) method with Log-rank test was performed to estimate survival probability
165 and the Cox proportional hazard model with a hazard ratio (HR) and 95% CI was executed for
166 statistical survival analysis. All analyses were carried out using GraphPad Prism (version 8.0). A
167 difference was considered statistically significant when P-value was less than 0.05. All studies
168 were conducted at least in triplicate unless otherwise specified.

169 **Results**

170 **NLRP3 agonist therapy is feasible but is ineffective alone and does not enhance the efficacy**
171 **of dual VEGFR2 and PD-1 blockade in orthotopic HCC models in mice with liver damage**

172 We first tested the feasibility and efficacy of NLRP3 alone or with dual VEGFR2 and PD-1
173 blockade in orthotopically grafted RIL-175 murine HCC in C57Bl/6 mice with underlying liver
174 damage. Mice with established tumors (approximately 5mm in diameter) were randomized to one
175 of the four treatment groups: **1)** NLRP3 agonist alone, **2)** anti-VEGFR2 (DC101) and anti-PD-
176 1(aPD-1) antibodies, **3)** NLRP3 agonist combined with anti-VEGFR2 and anti-PD-1 antibodies,
177 or **4)** isotype-matched IgG as a control. All treatments were administered for up to 5 weeks or until
178 mice became moribund (**Fig. 1A**). NLRP3 agonist-related toxicity was evidenced by transient
179 weight loss in the treated groups; the weight loss was less than the 15% limiting toxicity per the
180 animal protocol and all mice recovered 2 days after agent administration (**Fig. S1A**).

181 As expected, dual antibody blockade of VEGFR2 and PD-1 induced a significant tumor
182 growth delay in this model; in contrast, NLRP3 agonist alone was ineffective, and when combined
183 with dual DC101/anti-PD-1 antibody therapy did not affect tumor growth (**Figs. 1B & S1B**).
184 Similarly, we found a significant increase in median OS in tumor-bearing mice after DC101/anti-
185 PD-1 antibody therapy, but no significant difference between NLRP3 alone and control or triple
186 combination versus dual DC101/aPD-1 blockade alone (**Fig. 1C**). In addition to primary tumor
187 growth, mortality in this model can often be caused by the occurrence of ascites and pleural
188 effusions, and less frequently by peritoneal dissemination and lung metastases. Treatment with
189 NLRP3 agonist had no effect on these morbidities and did not impact the effects of dual
190 VEGFR2/PD-1 blockade on these parameters when added to the triple combination regimen (**Fig.**
191 **S1C-F**).

192 We next tested the feasibility and therapeutic efficacy of the NLRP3 agonist alone or
193 combined with dual VEGFR2 and PD-1 blockade in the HCA1 murine HCC model in C3H mice
194 with liver damage, which is resistant to anti-PD-1 therapy and highly metastatic to the lungs. As
195 seen in the RIL-175 model, treatment with NLRP3 agonist had acceptable toxicity but showed no
196 benefit when used alone or in combination with dual VEGFR2/PD-1 blockade (data not shown).

197 Thus, treatment with an NLRP3 agonist was feasible in mouse models of HCC with liver
198 damage, including in combination with VEGFR2 and anti-PD-1 antibodies, but did not confer any
199 additional benefits in reducing mortality or morbidity.

200 **NLRP3 agonist therapy is feasible but is ineffective alone and does not enhance the efficacy**
201 **of regorafenib and PD-1 blockade in orthotopic HCC models in mice with liver damage**

202 We first tested the feasibility and efficacy of the NLRP3 alone or with another effective
203 combination approach, using an intermediate dose of the multikinase inhibitor regorafenib
204 (10mg/kg q.d.) and PD-1 blockade in orthotopically grafted RIL-175 murine HCC models in mice
205 with underlying liver damage. Mice with established tumors (approximately 5mm in diameter)
206 were randomized to one of the four treatment groups: **1)** NLRP3 agonist alone, **2)** regorafenib and
207 anti-PD-1 antibody, **3)** NLRP3 agonist combined with regorafenib and anti-PD-1 antibody, or **4)**
208 isotype-matched IgG as a control. All treatments were administered for 3 weeks or until mice
209 became moribund (**Fig. 2A**). NLRP3 agonist and combination therapy with regorafenib/anti-PD-
210 1 antibody showed acceptable toxicity (weight loss less than 15%, and all mice recovered 2 days
211 after agent administration) (**Fig. S2A**).

212 As seen with dual antibody blockade of VEGFR2 and PD-1, NLRP3 agonist alone was
213 ineffective, and when combined with regorafenib/anti-PD-1 antibody therapy did not increase

214 tumor growth delay and tended to be inferior in terms of median OS compared to dual combination
215 alone (**Figs. 2B-C & S2B**). In addition, treatment with NLRP3 agonist did not reduce the incidence
216 of ascites, pleural effusions, peritoneal dissemination, or lung metastasis, when used alone or in
217 combination with regorafenib/anti-PD-1 therapy (**Fig. S2C-F**).

218 Thus, while treatment with an NLRP3 agonist in combination with regorafenib and anti-PD-1
219 antibody was feasible in mouse models of HCC with liver damage, it did not confer any benefits
220 in reducing mortality or morbidity.

221 **NLRP3 agonist therapy increased the expression of immune cytokines in blood circulation** 222 **but not in the tumor tissues**

223 We next set out to determine whether the lack of efficacy of the NLRP3 agonist was related
224 to the poor pharmacodynamic properties of the novel agent or due to unfavorable biological effects
225 in these models. To this end, we treated mice with established orthotopic RIL-175 murine HCCs
226 with NLRP3 agonist and sacrificed the mice after 4-hr and 24-hr to collect serial blood and tumor
227 tissue samples (**Fig. S3A**). Multiplexed protein array for pro-inflammatory cytokines was
228 performed for plasma and protein extracted from tumor samples to detect changes in the expression
229 level of pro-inflammatory cytokines. The results showed that mice treated with NLRP3 agonist
230 had significant and sustained increases in plasma levels of IL-1 β , IL-6, and KC/GRO, while
231 circulating levels of IFN- γ , IL-5, IL-10, and TNF- α were increased only after 4-hr but not after 24-
232 hr (**Fig. 3A**). We detected no differences in IL-2 or IL-12p70 at these time points (**Fig. S3B**).

233 In tumor tissues, only some of the changes were consistent with the treatment effects detected
234 in blood circulation. Specifically, intratumoral levels of IL-6 and KC/GRO were significantly
235 higher after 4-hr post-NLRP3 agonist treatment compared to control-treated mice. In contrast,

236 intratumoral levels of IL-1 β , IL-4, IL-5, and IL-10 were lower after 24-hr post-NLRP3 agonist
237 treatment, and IFN- γ and TNF- α levels were comparable at both time point (**Fig. 3B**). We also
238 used a multiplexed array for chemokine to measure changes in tumor tissues. We found higher
239 levels of IL-27p28 at both time-points and of CCL2 after 4-hr, and decreased IL-33 and CXCL10
240 levels after 24-hr post-NLRP3 agonist treatment compared to control-treated mice (**Fig. 3C**). There
241 were no differences in the expression levels of CCL-3, IL-9, or CXCL2 in tumors from the NLRP3
242 treated group at these time points (**Fig. S3C**).

243 In addition, we used the time-matched RNA extracted from HCC tissue samples to measure
244 changes after NLRP3 treatment in transcriptional levels of selected pro-inflammatory cytokines,
245 TAM and MDSC-related markers, and immune checkpoint molecules using qPCR assay. Among
246 pro-inflammatory cytokines, we found an increased transcriptional level of IFN- γ (both at 4-hr and
247 24-hr), TGFA (at 4-hr), and CXCL13 (at 24-hr) after treatment with the NLRP3 agonist (**Fig. 4A**).
248 Moreover, the expression levels of CSF1 (at 4-hr), IL-18 and CCL9, and PD-1, PD-L1, and CTLA-
249 4 (both at 4-hr and 24-hr) were up-regulated in samples from NLRP3 treatment group (**Fig. 4B-**
250 **C**). No changes were detected in the transcriptional levels of IL-1 β , IL-5, IL-6, IL-10, IFNA1,
251 CCR2, CXCL10, and CCL26 after NLRP3 agonist treatment at these time points (**Fig. S4**).

252 **Discussion**

253 New local and systemic treatments have recently become available for advanced HCC patients.
254 However, the increasing incidence of HCC globally and its aggressive progression and
255 refractoriness to treatment make it a persistent health and economic burden. Combination of
256 antiangiogenic drugs and ICB is now a standard modality, and many combinations of kinase
257 inhibitors with anti-PD-1 or anti-PD-L1 antibodies are in advanced stages of clinical development.
258 Based on available data, up to 30% of patients show a response (complete or partial) after these

259 combinational therapies, which in some cases is durable [15, 16, 34, 35]. Thus, despite the
260 impressive efficacy of this combinatorial approach, novel therapeutics are needed to safely extend
261 the benefits of these combinations.

262 In this study, we tested the feasibility and efficacy of a novel NLRP3 agonist in combination
263 with antiangiogenic agents and anti-PD-1 antibody. Our data confirmed that combining anti-
264 VEGFR2 and anti-PD1 antibodies or regorafenib and anti-PD1 antibodies is effective in murine
265 models, despite using different antibody types, treatment schedules, and suppliers in this study
266 compared to our prior reports [20, 21] . However, although some prior reports supported the
267 approach of targeting NLRP3 to enhance anti-tumor immunity in cancer, our results conclusively
268 demonstrate that this strategy, while feasible, was ineffective in murine HCC models with liver
269 damage [27, 36].

270 There are several potential explanations for the lack of efficacy for this approach in our models.
271 NLRP3 agonist therapy resulted in high circulating IL-1 β and intratumoral IL-18 levels. However,
272 these factors function as a double-edged sword by promoting tumor progression [26]. Indeed,
273 NLRP3 agonist therapy resulted in intratumoral changes at protein level consistent with increased
274 immunosuppression rather than immune activation. While in most contexts these changes did not
275 accelerate progression, there was a tendency for NLRP3 agonist therapy to compromise the
276 efficacy of multikinase inhibitor regorafenib with anti-PD-1 therapy. The immunosuppressive
277 factors included increases in IL-6, IL-10, KC/GRO, IL-27, CCL2, and IL-33 concentrations in
278 HCC tissue. Moreover, the level of CXCL10, a chemokine involved in effector T cell recruitment
279 in this model [21], was reduced by NLRP3 agonist therapy. Of note, expression levels of CSF-1
280 and CCL9 were increased at the transcriptional level after NLRP3 agonist therapy, along with
281 immune checkpoint molecules (PD-1, PD-L1, and CTLA-4), potentially indicating accumulation

282 or activation of myeloid cells (MDSCs and TAMs). Irrespective of the mechanisms involved, our
283 preclinical results do not support the use of this strategy alone or with antiangiogenic agents and
284 anti-PD-1 antibodies in HCC patients.

285 Future approaches will need to address two major unmet needs in ICB-based therapy for HCC.
286 One is addressing the profound immunosuppression in the microenvironment of advanced HCC,
287 which likely limits treatment efficacy. Another unmet need is developing approaches to directly
288 target the cancer cells as an approach to enhance the efficacy of ICB with antiangiogenic therapy.
289 To address these problems, multiple new strategies are being currently developed. For example,
290 we have recently shown that judicious scheduling of anti-PD-1 antibody with multikinase
291 inhibitors can show efficacy while reducing drug exposure [21]. Our prior work also demonstrated
292 the favorable reprogramming of the HCC microenvironment when anti-VEGFR and anti-PD-1
293 therapy was combined with CXCR4 inhibition [37]. Moreover, our group has also recently
294 demonstrated the efficacy of targeting HCC using p53 mRNA therapy to enhance the efficacy of
295 anti-PD-1 therapy [38]. Others have shown the potential therapeutic usefulness of targeting the
296 DNA-activated STING pathway combined with anti-PD-1 therapy in HCC [39]. There is
297 increasing interest in targeting innate or innate-like cells, recently reviewed in HCC [40], or gut
298 microbiome in HCC, as discussed by Schwabe RF et al [41]. Finally, many efforts are directed
299 toward the development of epigenetic modifiers such as HDAC inhibitors as immunomodulators
300 for ICB therapy in HCC models [42], and are currently being tested in clinical trials in other
301 cancers [43].

302 **Conclusions**

303 NLRP3 agonist showed acceptable toxicity but lacked efficacy in orthotopic murine HCC
304 models in mice with underlying liver damage and did not show any additional benefit when

305 combined with effective anti-PD-1/anti-angiogenic agents. While NLRP3 agonist therapy was
306 associated with pharmacodynamic increases in blood IL-1 β levels, the protein and transcriptional
307 analyses revealed an increase in immunosuppressive factors in the HCC tissues. Our preclinical
308 study data do not support the further development of NLRP3 agonists in HCC patients.

309 **Acknowledgments**

310 The authors would like to thank Mark Duquette, Anna Khachatryan, and Sylvie Roberge for
311 outstanding technical support.

312 **Author contributions**

313 **Conceptualization:** Dan G. Duda

314 **Data curation:** Dan G. Duda, Zhangya Pu

315 **Formal analysis:** Zhangya Pu

316 **Funding acquisition:** Dan G. Duda

317 **Investigation:** Zhangya Pu, Zelong Liu, Jiang Chen, Koetsu Inoue, Zhiping Ruan, Lingling Zhu,
318 Hiroto Kikuchi, Aya Matsui

319 **Project Administration:** Dan G. Duda

320 **Resources:** Peigen Huang

321 **Supervision:** Dan G. Duda

322 **Validation:** Zhangya Pu

323 **Visualization:** Zhangya Pu

324 **Writing – original draft preparation:** Zhangya Pu

325 **Writing – review & editing:** all authors

326 **Funding**

327 This study was supported through a sponsored research agreement with Bristol Meyer Squibb,
328 who provided funds and reagents (to DGD). DGD's research is supported through NIH grants
329 R01CA254351, R01CA260857, R01CA247441, P01CA261669, and R03CA256764, and
330 Department of Defense grants PRCRP W81XWH-19-1-0284 and PRCRP W81XWH-21-1-0738.

331 **Informed Consent Statement**

332 Not applicable.

333 **Data Availability Statement**

334 The original contributions presented in this study have been already included in the main text or
335 supplementary materials. For any inquiries, please contact the corresponding author.

336 **Conflict of Interest Disclosure**

337 DGD received consultant fees from Innocoll and research grants from Exelixis and Surface
338 Oncology. No reagents from these companies were used in this study.

339 **Figure legend**

340 **Fig 1. Therapeutic efficacy of NLRP3 agonist alone or combined with anti-PD-1 (aPD-1) and**
341 **anti-VEGFR2 (DC101) antibodies in orthotopic murine HCC in C57Bl/6 mice. (A)** Study
342 design. Before intrahepatic implantation of RIL-175 cells, C57Bl/6 mice were treated with CCl4
343 by gavage for 12 weeks to induce liver damage. **(B, C)** Tumor growth kinetics **(B)** and overall
344 survival distributions **(C)** in the four treatment groups (n=15 mice/group). P values from one-way
345 ANOVA with a Brown-Forsythe test **(B)** and log-rank test **(C)**. ** P<0.01, **** P<0.0001, ns: not
346 significant.

347 **Fig 2. Therapeutic efficacy of NLRP3 agonist alone or combined with anti-PD-1 (aPD-1) and**
348 **regorafenib (rego) in orthotopic murine HCC in C57Bl/6 mice. (A)** Study design. Before
349 intrahepatic implantation of RIL-175 cells, C57Bl/6 mice were treated with CCl4 by gavage for
350 12 weeks to induce liver damage. **(B, C)** Tumor growth kinetics **(B)** and overall survival
351 distributions **(C)** in the four treatment groups (n=15 mice/group). P values from one-way ANOVA
352 with a Brown-Forsythe test **(B)** and log-rank test **(C)**. ** P<0.01, **** P<0.0001, ns: not
353 significant.

354 **Fig 3. Systemic and intratumoral changes in cytokine/chemokine expression level changed**
355 **after NLRP3 agonist treatment in mice with orthotopic murine HCC in C57Bl/6 mice. (A-C)**
356 Multiplexed array measurements of cytokines and chemokines in plasma **(A)** and tumor tissues
357 **(B, C)** at 4 hr and 24 hr after NLRP3 agonist treatment (n=6-7 mice/group). P values from one-
358 way ANOVA with a Brown-Forsythe test. * P<0.05; ** P<0.01, *** P<0.001, **** P<0.0001, ns:
359 not significant.

360 **Fig 4. Intratumoral changes in expression levels of selected immunomodulatory genes after**
361 **NLRP3 agonist treatment in mice with orthotopic murine HCC in C57Bl/6 mice. (A-C)**
362 Quantitative PCR measurements of proinflammatory factors (IFN- γ , TGFA, CXCL13) (**A**), tumor-
363 associated macrophage (TAM) (CSF1) and myeloid-derived-suppressor cell (MDSC) markers (IL-
364 18, CCL9) (**B**), and immune checkpoint molecules (PD-1, PD-L1, CTLA-4) (**C**), at 4hr and 24 hr
365 after NLRP3 agonist treatment (n=6-7 mice/group). P values from one-way ANOVA with a
366 Brown-Forsythe test. * P<0.05; ** P<0.01, ns: not significant.

367 **References**

- 368 1. Forner A, Reig M, Bruix J. Hepatocellular carcinoma. *Lancet* (London, England).
369 2018;391(10127):1301-14. Epub 2018/01/09. doi: 10.1016/s0140-6736(18)30010-2.
370 PubMed PMID: 29307467.
- 371 2. Llovet JM, Kelley RK, Villanueva A, Singal AG, Pikarsky E, Roayaie S, et al.
372 Hepatocellular carcinoma. *Nat Rev Dis Primers*. 2021;7(1):6. Epub 2021/01/23. doi:
373 10.1038/s41572-020-00240-3. PubMed PMID: 33479224.
- 374 3. Kudo M, Kawamura Y, Hasegawa K, Tateishi R, Kariyama K, Shiina S, et al. Management
375 of Hepatocellular Carcinoma in Japan: JSH Consensus Statements and Recommendations
376 2021 Update. *Liver Cancer*. 2021;10(3):181-223. Epub 2021/07/10. doi:
377 10.1159/000514174. PubMed PMID: 34239808; PubMed Central PMCID:
378 PMC8237791.
- 379 4. Kulik L, El-Serag HB. Epidemiology and Management of Hepatocellular Carcinoma.
380 *Gastroenterology*. 2019;156(2):477-91 e1. Epub 2018/10/28. doi:
381 10.1053/j.gastro.2018.08.065. PubMed PMID: 30367835; PubMed Central PMCID:
382 PMC6340716.
- 383 5. Lawal G, Xiao Y, Rahnemai-Azar AA, Tsilimigras DI, Kuang M, Bakopoulos A, et al. The
384 Immunology of Hepatocellular Carcinoma. *Vaccines*. 2021;9(10). Epub 2021/10/27. doi:
385 10.3390/vaccines9101184. PubMed PMID: 34696292; PubMed Central PMCID:
386 PMC8538643.
- 387 6. Sia D, Jiao Y, Martinez-Quetglas I, Kuchuk O, Villacorta-Martin C, Castro de Moura M,
388 et al. Identification of an Immune-specific Class of Hepatocellular Carcinoma, Based on

- 389 Molecular Features. *Gastroenterology*. 2017;153(3):812-26. Epub 2017/06/19. doi:
390 10.1053/j.gastro.2017.06.007. PubMed PMID: 28624577.
- 391 7. Li X, Ramadori P, Pfister D, Seehawer M, Zender L, Heikenwalder M. The immunological
392 and metabolic landscape in primary and metastatic liver cancer. *Nat Rev Cancer*.
393 2021;21(9):541-57. Epub 2021/07/31. doi: 10.1038/s41568-021-00383-9. PubMed PMID:
394 34326518.
- 395 8. Lu C, Rong D, Zhang B, Zheng W, Wang X, Chen Z, et al. Current perspectives on the
396 immunosuppressive tumor microenvironment in hepatocellular carcinoma: challenges and
397 opportunities. *Mol Cancer*. 2019;18(1):130. Epub 2019/08/30. doi: 10.1186/s12943-019-
398 1047-6. PubMed PMID: 31464625; PubMed Central PMCID: PMC6714090.
- 399 9. Seehawer M, Heinzmann F, D'Artista L, Harbig J, Roux PF, Hoenicke L, et al. Necroptosis
400 microenvironment directs lineage commitment in liver cancer. *Nature*. 2018;562(7725):69-
401 75. Epub 2018/09/14. doi: 10.1038/s41586-018-0519-y. PubMed PMID: 30209397;
402 PubMed Central PMCID: PMC68111790.
- 403 10. Zheng C, Zheng L, Yoo JK, Guo H, Zhang Y, Guo X, et al. Landscape of Infiltrating T
404 Cells in Liver Cancer Revealed by Single-Cell Sequencing. *Cell*. 2017;169(7):1342-56.e16.
405 Epub 2017/06/18. doi: 10.1016/j.cell.2017.05.035. PubMed PMID: 28622514.
- 406 11. Zheng Y, Wang S, Cai J, Ke A, Fan J. The progress of immune checkpoint therapy in
407 primary liver cancer. *Biochimica et biophysica acta Reviews on cancer*.
408 2021;1876(2):188638. Epub 2021/10/25. doi: 10.1016/j.bbcan.2021.188638. PubMed
409 PMID: 34688805.
- 410 12. Yuan D, Huang S, Berger E, Liu L, Gross N, Heinzmann F, et al. Kupffer Cell-Derived
411 Tnf Triggers Cholangiocellular Tumorigenesis through JNK due to Chronic Mitochondrial

- 412 Dysfunction and ROS. *Cancer cell*. 2017;31(6):771-89.e6. Epub 2017/06/14. doi:
413 10.1016/j.ccell.2017.05.006. PubMed PMID: 28609656; PubMed Central PMCID:
414 PMCPMC7909318.
- 415 13. El-Khoueiry AB, Sangro B, Yau T, Crocenzi TS, Kudo M, Hsu C, et al. Nivolumab in
416 patients with advanced hepatocellular carcinoma (CheckMate 040): an open-label, non-
417 comparative, phase 1/2 dose escalation and expansion trial. *Lancet (London, England)*.
418 2017;389(10088):2492-502. Epub 2017/04/25. doi: 10.1016/s0140-6736(17)31046-2.
419 PubMed PMID: 28434648; PubMed Central PMCID: PMCPMC7539326.
- 420 14. Zhu AX, Finn RS, Edeline J, Cattan S, Ogasawara S, Palmer D, et al. Pembrolizumab in
421 patients with advanced hepatocellular carcinoma previously treated with sorafenib
422 (KEYNOTE-224): a non-randomised, open-label phase 2 trial. *The Lancet Oncology*.
423 2018;19(7):940-52. Epub 2018/06/08. doi: 10.1016/s1470-2045(18)30351-6. PubMed
424 PMID: 29875066.
- 425 15. Albini A, Bruno A, Noonan DM, Mortara L. Contribution to Tumor Angiogenesis From
426 Innate Immune Cells Within the Tumor Microenvironment: Implications for
427 Immunotherapy. *Front Immunol*. 2018;9:527. Epub 2018/04/21. doi:
428 10.3389/fimmu.2018.00527. PubMed PMID: 29675018; PubMed Central PMCID:
429 PMCPMC5895776.
- 430 16. Lee WS, Yang H, Chon HJ, Kim C. Combination of anti-angiogenic therapy and immune
431 checkpoint blockade normalizes vascular-immune crosstalk to potentiate cancer immunity.
432 *Exp Mol Med*. 2020;52(9):1475-85. Epub 2020/09/12. doi: 10.1038/s12276-020-00500-y.
433 PubMed PMID: 32913278; PubMed Central PMCID: PMCPMC8080646.

- 434 17. Finn RS, Ryoo BY, Merle P, Kudo M, Bouattour M, Lim HY, et al. Pembrolizumab As
435 Second-Line Therapy in Patients With Advanced Hepatocellular Carcinoma in
436 KEYNOTE-240: A Randomized, Double-Blind, Phase III Trial. *Journal of clinical
437 oncology : official journal of the American Society of Clinical Oncology*. 2020;38(3):193-
438 202. Epub 2019/12/04. doi: 10.1200/jco.19.01307. PubMed PMID: 31790344.
- 439 18. Yau T, Park JW, Finn RS, Cheng AL, Mathurin P, Edeline J, et al. CheckMate 459: A
440 randomized, multi-center phase III study of nivolumab (NIVO) vs sorafenib (SOR) as first-
441 line (1L) treatment in patients (pts) with advanced hepatocellular carcinoma (aHCC).
442 *Annals of Oncology*. 2019;30:v874-v5. doi: 10.1093/annonc/mdz394.029.
- 443 19. Fukumura D, Kloepper J, Amoozgar Z, Duda DG, Jain RK. Enhancing cancer
444 immunotherapy using antiangiogenics: opportunities and challenges. *Nat Rev Clin Oncol*.
445 2018;15(5):325-40. Epub 2018/03/07. doi: 10.1038/nrclinonc.2018.29. PubMed PMID:
446 29508855; PubMed Central PMCID: PMC5921900.
- 447 20. Shigeta K, Datta M, Hato T, Kitahara S, Chen IX, Matsui A, et al. Dual Programmed Death
448 Receptor-1 and Vascular Endothelial Growth Factor Receptor-2 Blockade Promotes
449 Vascular Normalization and Enhances Antitumor Immune Responses in Hepatocellular
450 Carcinoma. *Hepatology*. 2020;71(4):1247-61. Epub 2019/08/06. doi: 10.1002/hep.30889.
451 PubMed PMID: 31378984; PubMed Central PMCID: PMC7000304.
- 452 21. Shigeta K, Matsui A, Kikuchi H, Klein S, Mamessier E, Chen IX, et al. Regorafenib
453 combined with PD1 blockade increases CD8 T-cell infiltration by inducing CXCL10
454 expression in hepatocellular carcinoma. *J Immunother Cancer*. 2020;8(2). Epub
455 2020/11/26. doi: 10.1136/jitc-2020-001435. PubMed PMID: 33234602; PubMed Central
456 PMCID: PMC7689089.

- 457 22. Finn RS, Qin S, Ikeda M, Galle PR, Ducreux M, Kim TY, et al. Atezolizumab plus
458 Bevacizumab in Unresectable Hepatocellular Carcinoma. *N Engl J Med*.
459 2020;382(20):1894-905. Epub 2020/05/14. doi: 10.1056/NEJMoa1915745. PubMed
460 PMID: 32402160.
- 461 23. Pinter M, Jain RK, Duda DG. The Current Landscape of Immune Checkpoint Blockade in
462 Hepatocellular Carcinoma: A Review. *JAMA oncology*. 2021;7(1):113-23. Epub
463 2020/10/23. doi: 10.1001/jamaoncol.2020.3381. PubMed PMID: 33090190; PubMed
464 Central PMCID: PMC8265820.
- 465 24. Fu Y, Liu S, Zeng S, Shen H. From bench to bed: the tumor immune microenvironment
466 and current immunotherapeutic strategies for hepatocellular carcinoma. *J Exp Clin Cancer*
467 *Res*. 2019;38(1):396. Epub 2019/09/11. doi: 10.1186/s13046-019-1396-4. PubMed PMID:
468 31500650; PubMed Central PMCID: PMC6734524.
- 469 25. Oura K, Morishita A, Tani J, Masaki T. Tumor Immune Microenvironment and
470 Immunosuppressive Therapy in Hepatocellular Carcinoma: A Review. *International*
471 *journal of molecular sciences*. 2021;22(11). Epub 2021/06/03. doi: 10.3390/ijms22115801.
472 PubMed PMID: 34071550; PubMed Central PMCID: PMC8198390.
- 473 26. Hamarshah S, Zeiser R. NLRP3 Inflammasome Activation in Cancer: A Double-Edged
474 Sword. *Front Immunol*. 2020;11:1444. Epub 2020/08/01. doi: 10.3389/fimmu.2020.01444.
475 PubMed PMID: 32733479; PubMed Central PMCID: PMC7360837.
- 476 27. Moossavi M, Parsamanesh N, Bahrami A, Atkin SL, Sahebkar A. Role of the NLRP3
477 inflammasome in cancer. *Mol Cancer*. 2018;17(1):158. Epub 2018/11/19. doi:
478 10.1186/s12943-018-0900-3. PubMed PMID: 30447690; PubMed Central PMCID:
479 PMC6240225.

- 480 28. Wang H, Wang Y, Du Q, Lu P, Fan H, Lu J, et al. Inflammasome-independent NLRP3 is
481 required for epithelial-mesenchymal transition in colon cancer cells. *Experimental cell*
482 *research*. 2016;342(2):184-92. Epub 2016/03/13. doi: 10.1016/j.yexcr.2016.03.009.
483 PubMed PMID: 26968633.
- 484 29. Wei Q, Mu K, Li T, Zhang Y, Yang Z, Jia X, et al. Deregulation of the NLRP3
485 inflammasome in hepatic parenchymal cells during liver cancer progression. *Laboratory*
486 *investigation; a journal of technical methods and pathology*. 2014;94(1):52-62. Epub
487 2013/10/30. doi: 10.1038/labinvest.2013.126. PubMed PMID: 24166187.
- 488 30. Fan SH, Wang YY, Lu J, Zheng YL, Wu DM, Li MQ, et al. Luteoloside suppresses
489 proliferation and metastasis of hepatocellular carcinoma cells by inhibition of NLRP3
490 inflammasome. *PloS one*. 2014;9(2):e89961. Epub 2014/03/04. doi:
491 10.1371/journal.pone.0089961. PubMed PMID: 24587153; PubMed Central PMCID:
492 PMCPMC3935965.
- 493 31. Tofilon PJ, Basic I, Milas L. Prediction of in vivo tumor response to chemotherapeutic
494 agents by the in vitro sister chromatid exchange assay. *Cancer research*. 1985;45(5):2025-
495 30. Epub 1985/05/01. PubMed PMID: 4039220.
- 496 32. Chen Y, Huang Y, Reiberger T, Duyverman AM, Huang P, Samuel R, et al. Differential
497 effects of sorafenib on liver versus tumor fibrosis mediated by stromal-derived factor 1
498 alpha/C-X-C receptor type 4 axis and myeloid differentiation antigen-positive myeloid cell
499 infiltration in mice. *Hepatology*. 2014;59(4):1435-47. Epub 2013/11/19. doi:
500 10.1002/hep.26790. PubMed PMID: 24242874; PubMed Central PMCID:
501 PMCPMC3966948.

- 502 33. Reiberger T, Chen Y, Ramjiawan RR, Hato T, Fan C, Samuel R, et al. An orthotopic mouse
503 model of hepatocellular carcinoma with underlying liver cirrhosis. *Nature protocols*.
504 2015;10(8):1264-74. Epub 2015/07/24. doi: 10.1038/nprot.2015.080. PubMed PMID:
505 26203823; PubMed Central PMCID: PMC4800979.
- 506 34. Bertuccio P, Turati F, Carioli G, Rodriguez T, La Vecchia C, Malvezzi M, et al. Global
507 trends and predictions in hepatocellular carcinoma mortality. *Journal of hepatology*.
508 2017;67(2):302-9. Epub 2017/03/25. doi: 10.1016/j.jhep.2017.03.011. PubMed PMID:
509 28336466.
- 510 35. Kole C, Charalampakis N, Tsakatikas S, Vailas M, Moris D, Gkotsis E, et al.
511 Immunotherapy for Hepatocellular Carcinoma: A 2021 Update. *Cancers (Basel)*.
512 2020;12(10). Epub 2020/10/07. doi: 10.3390/cancers12102859. PubMed PMID: 33020428;
513 PubMed Central PMCID: PMC4800979.
- 514 36. Lu F, Zhao Y, Pang Y, Ji M, Sun Y, Wang H, et al. NLRP3 inflammasome upregulates
515 PD-L1 expression and contributes to immune suppression in lymphoma. *Cancer Lett*.
516 2021;497:178-89. Epub 2020/10/23. doi: 10.1016/j.canlet.2020.10.024. PubMed PMID:
517 33091534.
- 518 37. Chen Y, Ramjiawan RR, Reiberger T, Ng MR, Hato T, Huang Y, et al. CXCR4 inhibition
519 in tumor microenvironment facilitates anti-programmed death receptor-1 immunotherapy
520 in sorafenib-treated hepatocellular carcinoma in mice. *Hepatology*. 2015;61(5):1591-602.
521 Epub 2014/12/23. doi: 10.1002/hep.27665. PubMed PMID: 25529917; PubMed Central
522 PMCID: PMC4406806.
- 523 38. Xiao Y, Chen J, Zhou H, Zeng X, Ruan Z, Pu Z, et al. Combining p53 mRNA nanotherapy
524 with immune checkpoint blockade reprograms the immune microenvironment for effective

- 525 cancer therapy. *Nature communications*. 2022;13(1):758. Epub 2022/02/11. doi:
526 10.1038/s41467-022-28279-8. PubMed PMID: 35140208.
- 527 39. Thomsen MK, Skouboe MK, Boularan C, Vernejoul F, Lioux T, Leknes SL, et al. The
528 cGAS-STING pathway is a therapeutic target in a preclinical model of hepatocellular
529 carcinoma. *Oncogene*. 2020;39(8):1652-64. Epub 2019/11/20. doi: 10.1038/s41388-019-
530 1108-8. PubMed PMID: 31740782.
- 531 40. Ruf B, Heinrich B, Greten TF. Immunobiology and immunotherapy of HCC: spotlight on
532 innate and innate-like immune cells. *Cellular & molecular immunology*. 2021;18(1):112-
533 27. Epub 2020/11/26. doi: 10.1038/s41423-020-00572-w. PubMed PMID: 33235387;
534 PubMed Central PMCID: PMC7852696.
- 535 41. Schwabe RF, Greten TF. Gut microbiome in HCC - Mechanisms, diagnosis and therapy.
536 *Journal of hepatology*. 2020;72(2):230-8. Epub 2020/01/20. doi:
537 10.1016/j.jhep.2019.08.016. PubMed PMID: 31954488.
- 538 42. Llopiz D, Ruiz M, Villanueva L, Iglesias T, Silva L, Egea J, et al. Enhanced anti-tumor
539 efficacy of checkpoint inhibitors in combination with the histone deacetylase inhibitor
540 Belinostat in a murine hepatocellular carcinoma model. *Cancer immunology,
541 immunotherapy : CII*. 2019;68(3):379-93. Epub 2018/12/14. doi: 10.1007/s00262-018-
542 2283-0. PubMed PMID: 30547218.
- 543 43. Ny L, Jespersen H, Karlsson J, Alsén S, Filges S, All-Eriksson C, et al. The PEMDAC
544 phase 2 study of pembrolizumab and entinostat in patients with metastatic uveal melanoma.
545 *Nature communications*. 2021;12(1):5155. Epub 2021/08/29. doi: 10.1038/s41467-021-
546 25332-w. PubMed PMID: 34453044; PubMed Central PMCID: PMC78397717.
- 547

548 **Supporting information**

549 **Fig. S1: Effects of NLRP3 agonist alone or combined with anti-PD-1 (aPD-1) and anti-**
550 **VEGFR2 (DC101) antibodies in orthotopic murine HCC in C57Bl/6 mice. A** Changes in body
551 of mice during treatment in the overall cohorts and in individual mice in the four treatment groups
552 (n=15 mice/group). **B** The tumor volume curve in individual mice. **C-F** Incidence of ascites **C**,
553 pleural effusion **D**, lung metastasis **E**, and peritoneal dissemination **F** in the in the four treatment
554 groups (n=15 mice/group).

555 **Fig. S2: Effects of NLRP3 agonist alone or combined with anti-PD-1 (aPD-1) and regorafenib**
556 **(rego) in orthotopic murine HCC in C57Bl/6 mice. A** Changes in body of mice during treatment
557 in the overall cohorts and in individual mice in the four treatment groups (n=15 mice/group). **B**
558 The tumor volume curve in individual mice. **C-F** Incidence of ascites **C**, pleural effusion **D**, lung
559 metastasis **E**, and peritoneal dissemination **F** in the in the four treatment groups (n=15 mice/group).

560 **Fig. S3: Systemic and intratumoral changes in cytokine/chemokine expression level after**
561 **NLRP3 agonist treatment in mice with orthotopic murine HCC in C57Bl/6 mice. A**
562 Experimental design. **B, C** Multiplexed array measurements of cytokines and chemokines in
563 plasma **B** and tumor tissues (**B and C**) at 4hr and 24 hr after NLRP3 agonist treatment. Statistical
564 analysis using one-way ANOVA with a Brown-Forsythe test, ns: not significant.

565 **Fig. S4: Intratumoral changes in expression levels of immunomodulatory genes after NLRP3**
566 **agonist treatment in mice with orthotopic murine HCC in C57Bl/6 mice.** Quantitative PCR
567 measurements of proinflammatory factors (IL-1 β , IL-5, IL-6, IL-10, IFNA1), tumor-associated
568 macrophage (TAM) (CCR2, CXCL10) and myeloid-derived-suppressor cells (MDSC) (CCL26)
569 markers at 4hr and 24 hr after NLRP3 agonist treatment (n=6-7 mice/group). Statistical analysis
570 using one-way ANOVA with a Brown-Forsythe test, ns: not significant.

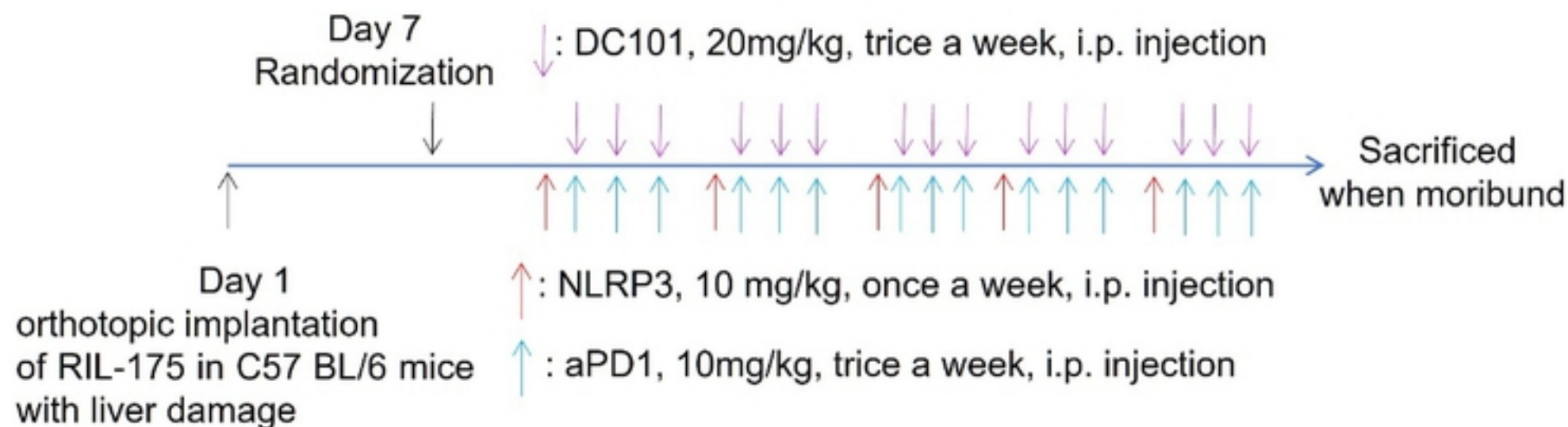
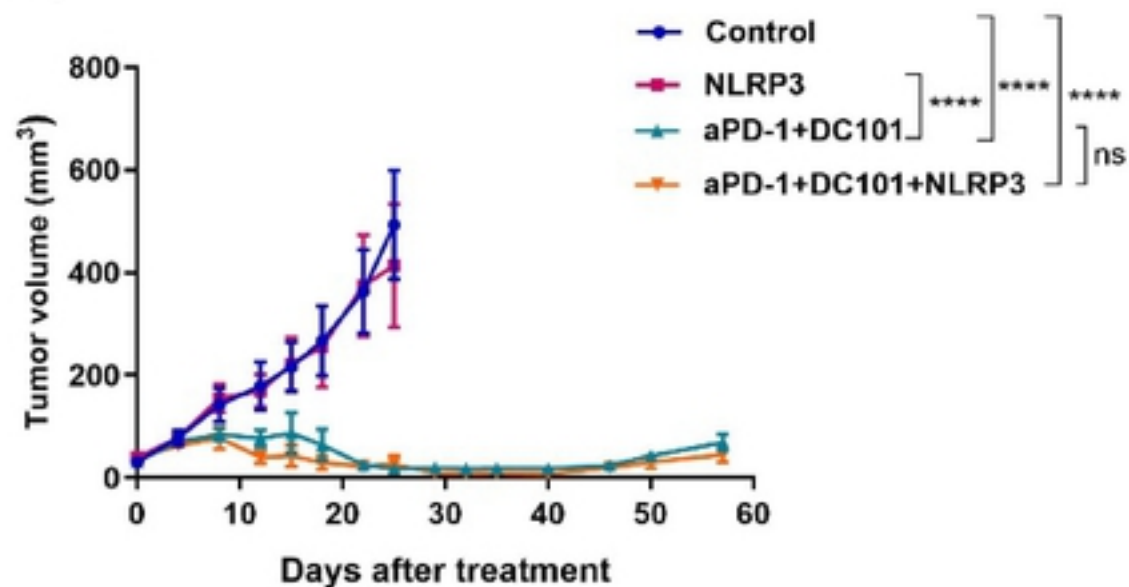
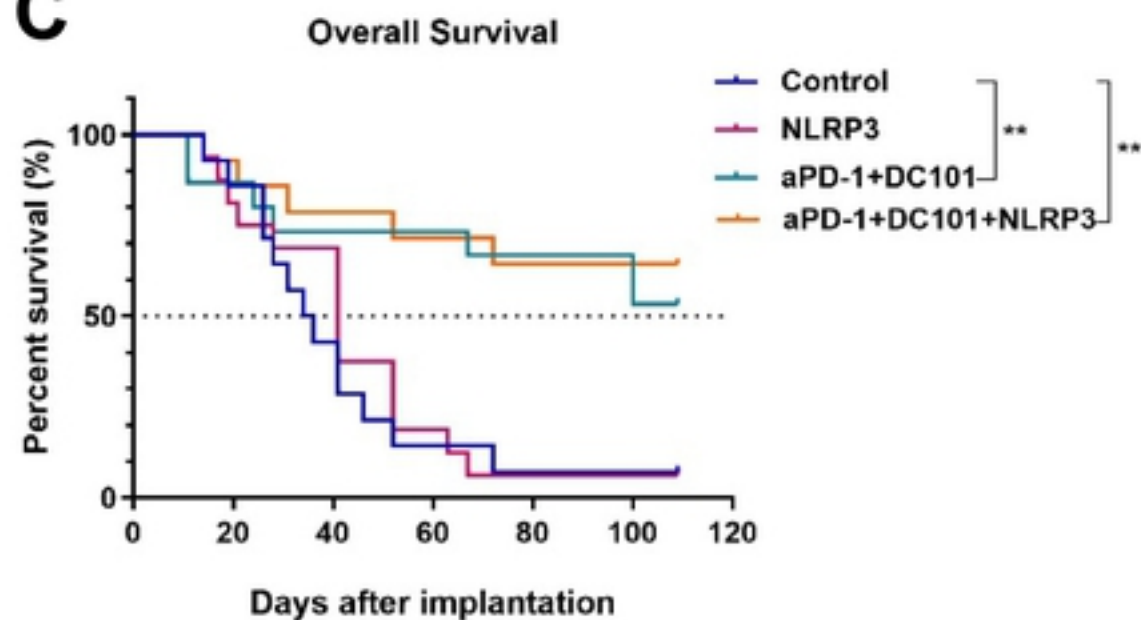
A**Treatment for 5 weeks****B****C**

Figure 1

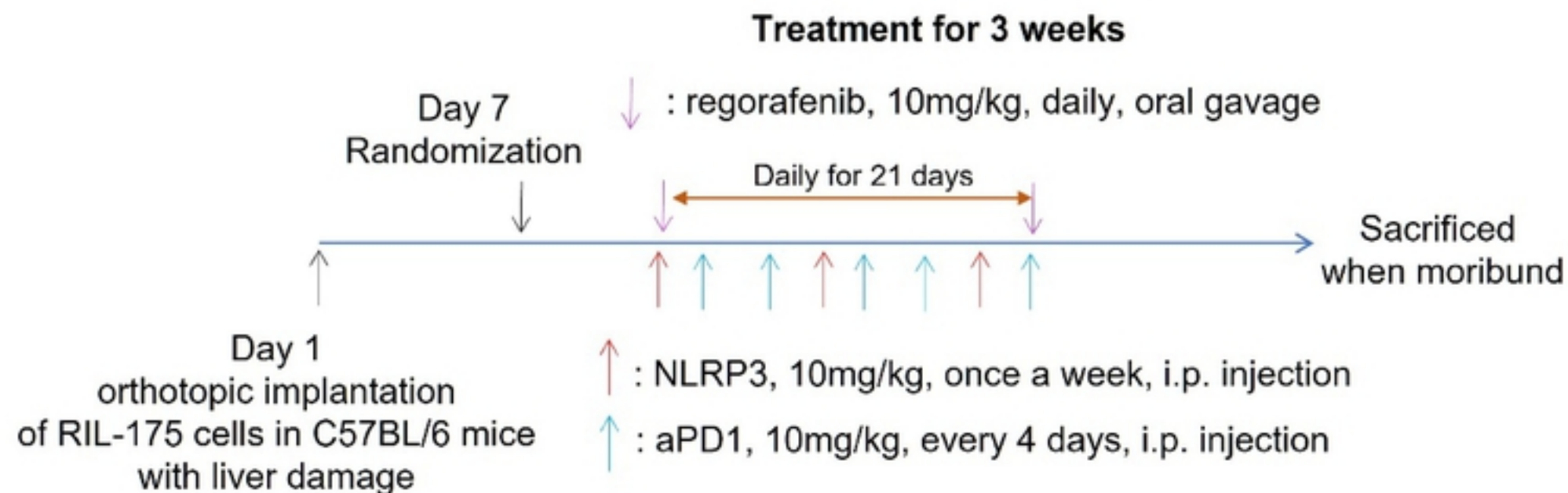
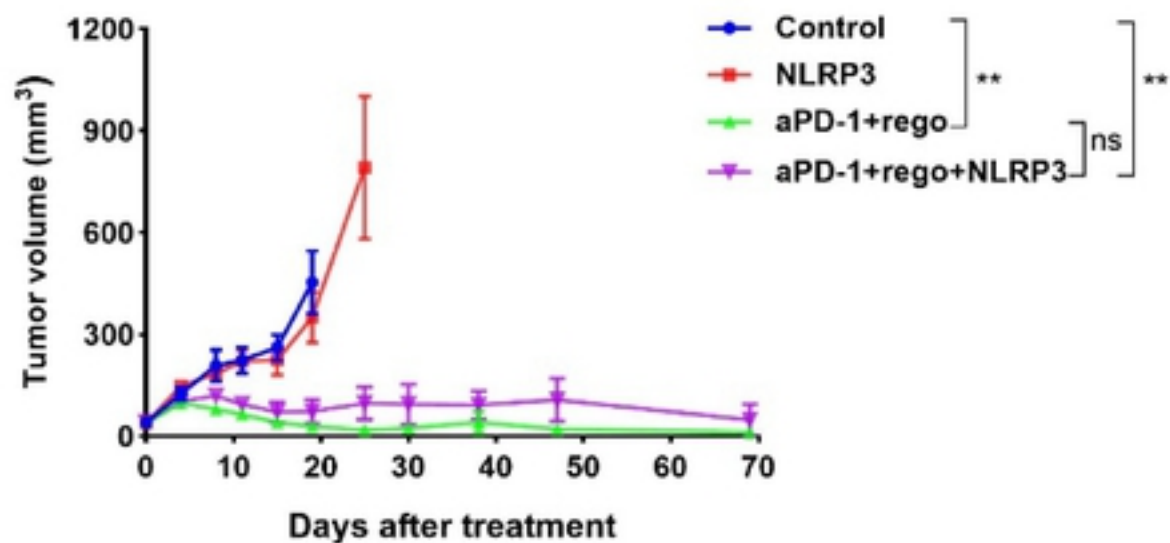
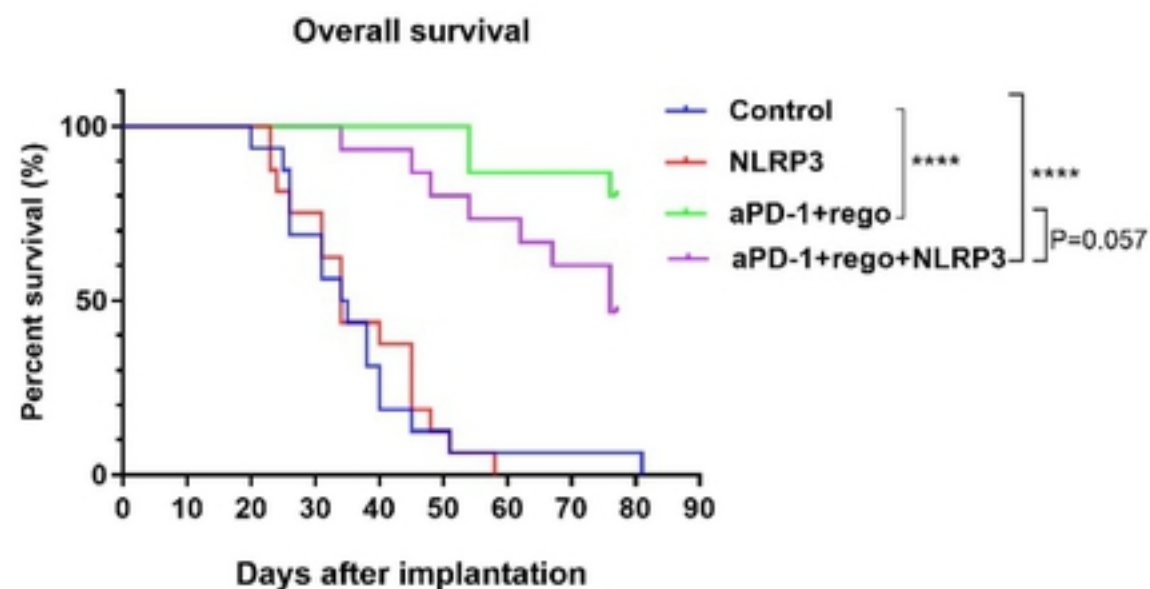
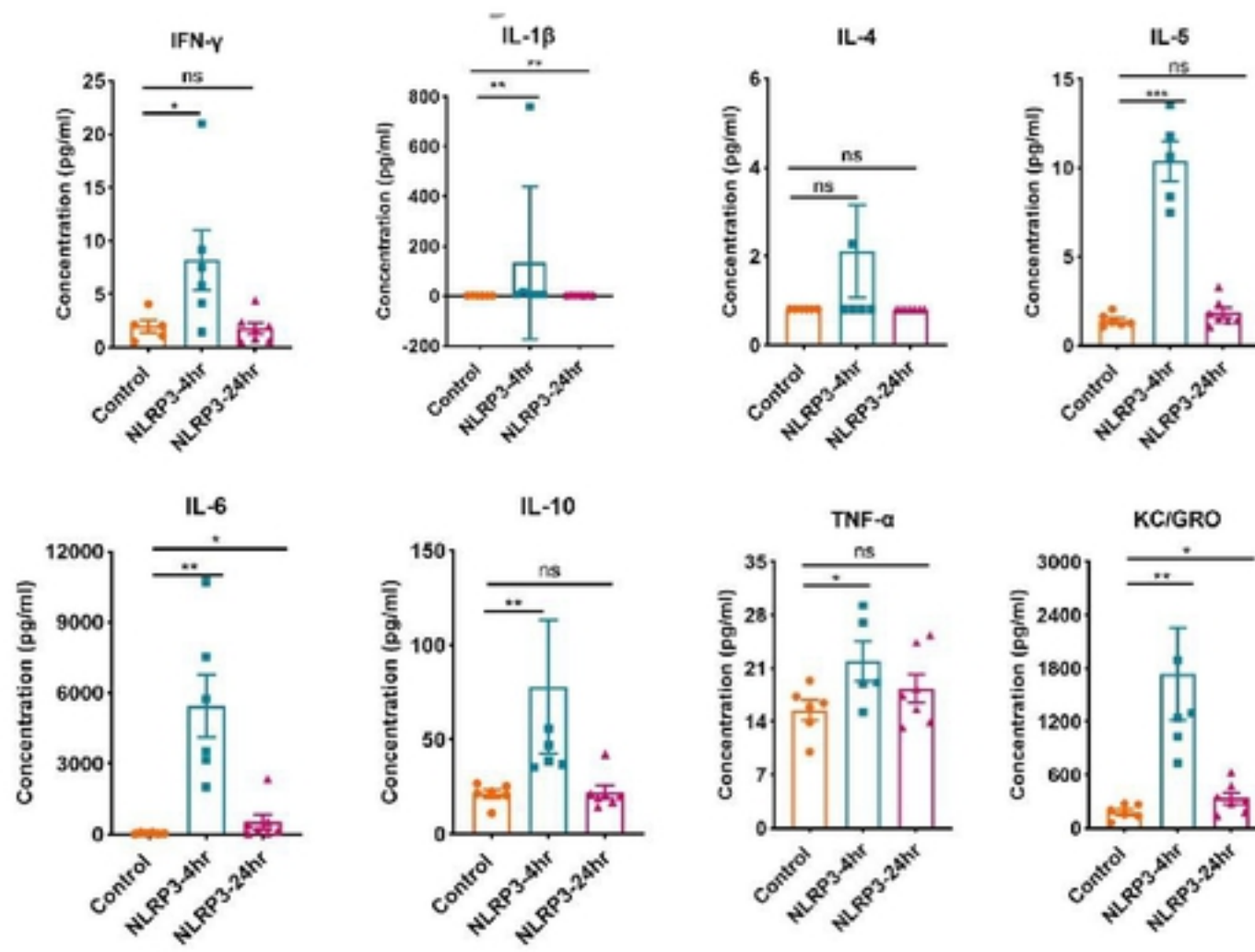
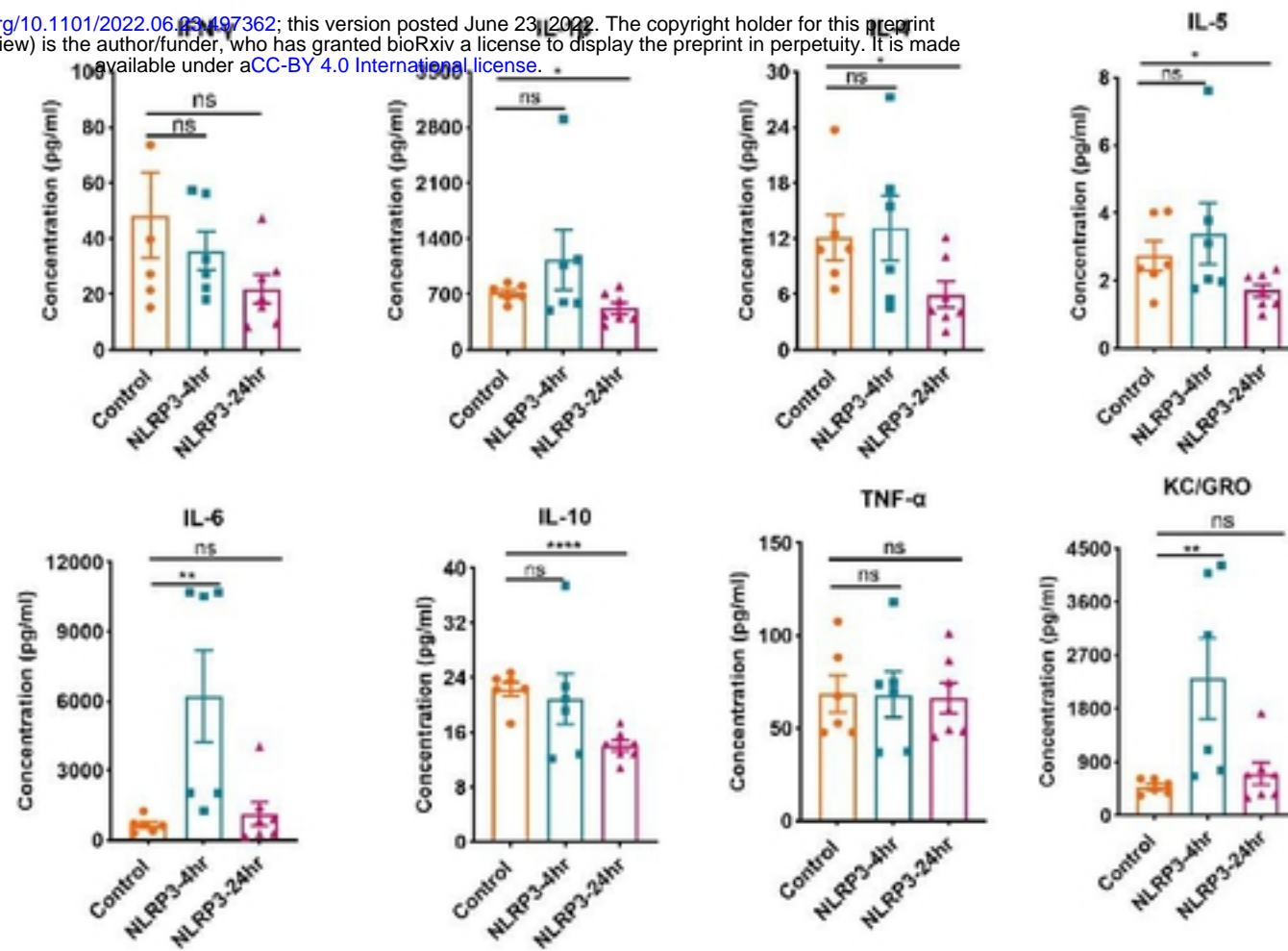
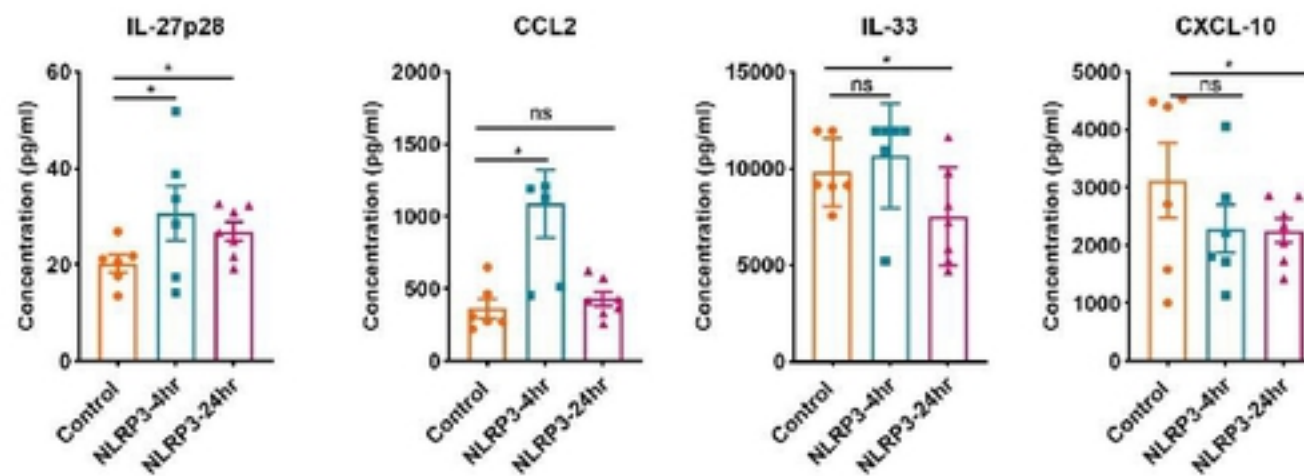
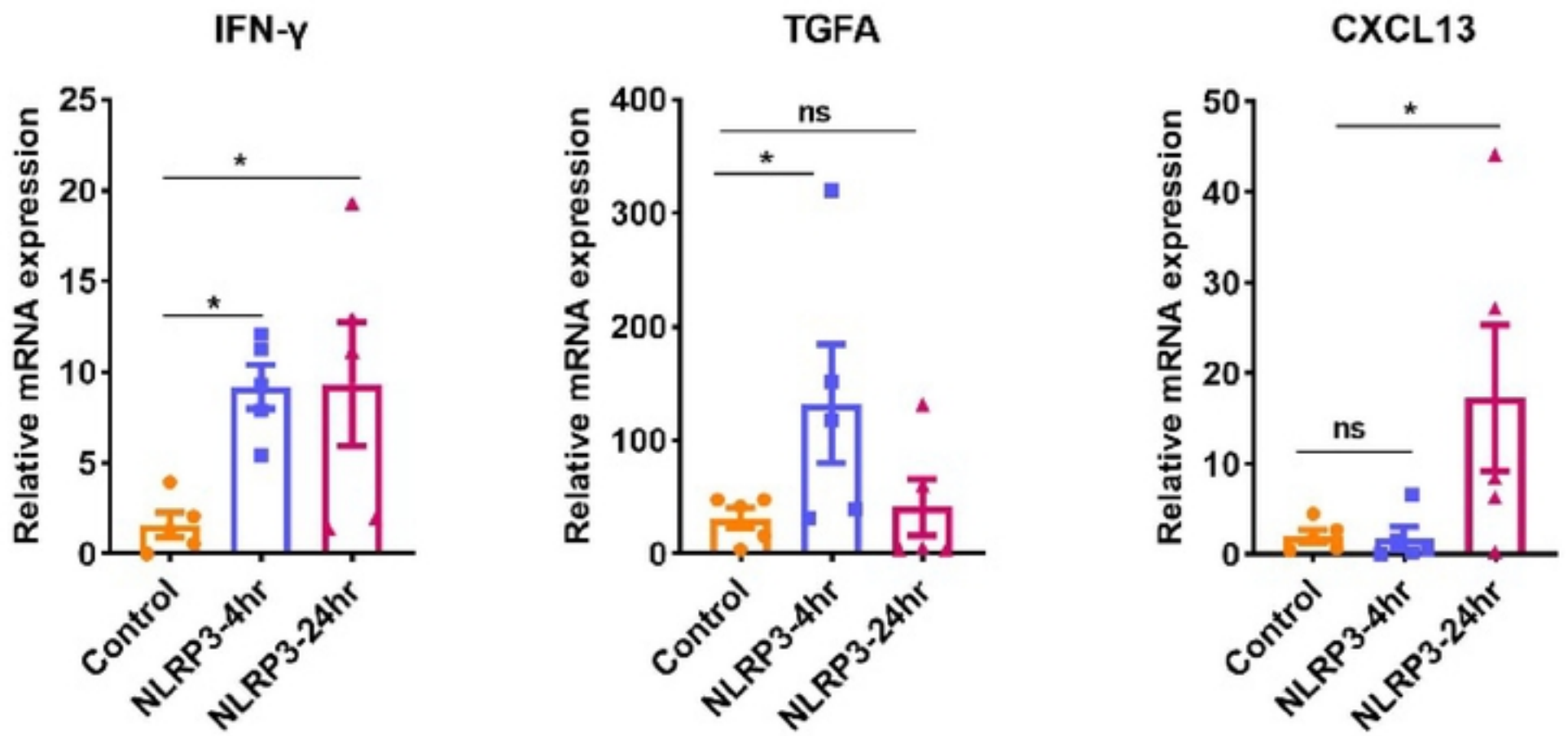
A**B****C**

Figure 2

A**Plasma**

bioRxiv preprint doi: <https://doi.org/10.1101/2022.06.03.497362>; this version posted June 23, 2022. The copyright holder for this preprint (which was not certified by peer review) is the author/funder, who has granted bioRxiv a license to display the preprint in perpetuity. It is made available under aCC-BY 4.0 International license.

B**Tumor****C****Tumor**

A**B**

bioRxiv preprint doi: <https://doi.org/10.1101/2022.06.23.497362>; this version posted June 23, 2022. The copyright holder for this preprint (which was not certified by peer review) is the author/funder, who has granted bioRxiv a license to display the preprint in perpetuity. It is made available under aCC-BY 4.0 International license.

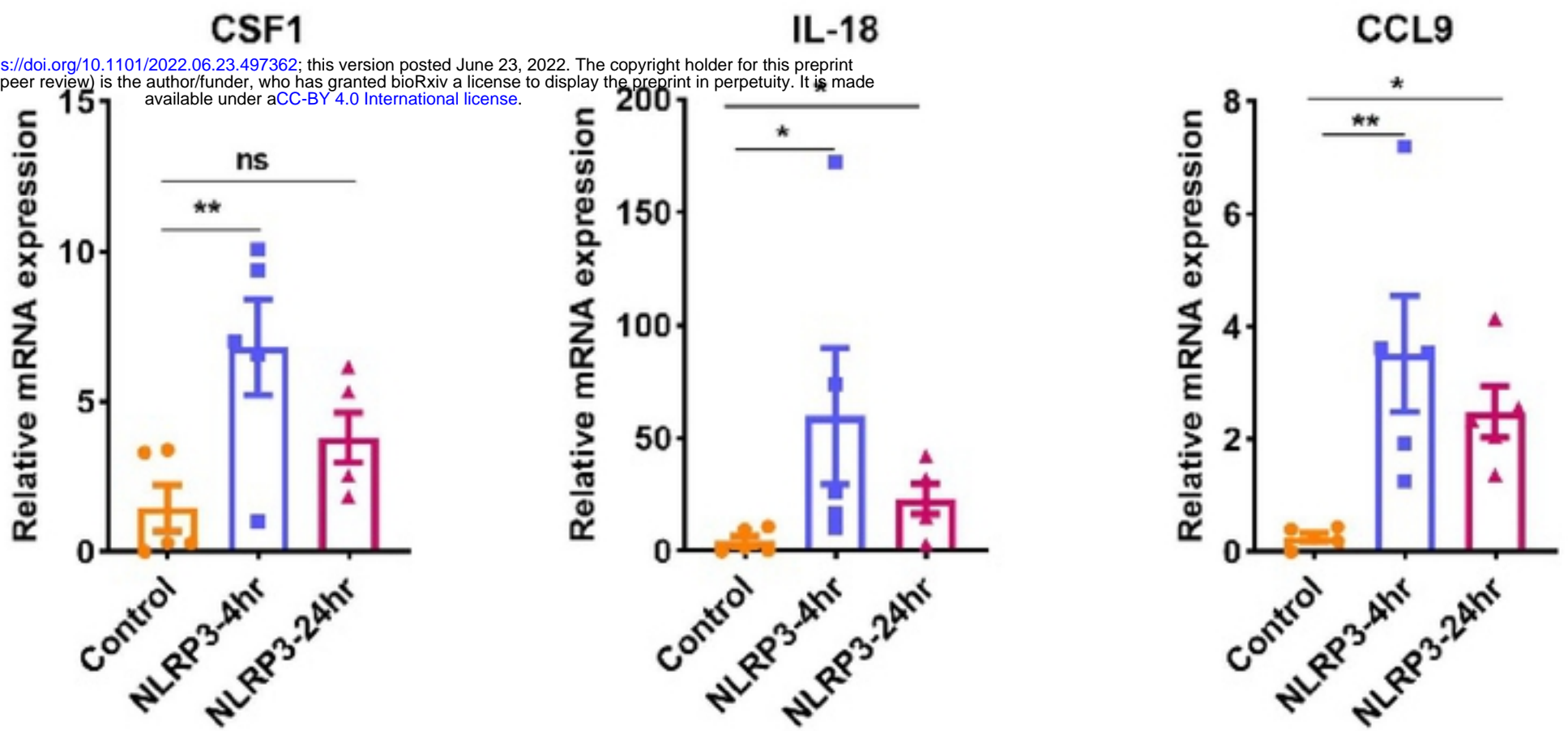
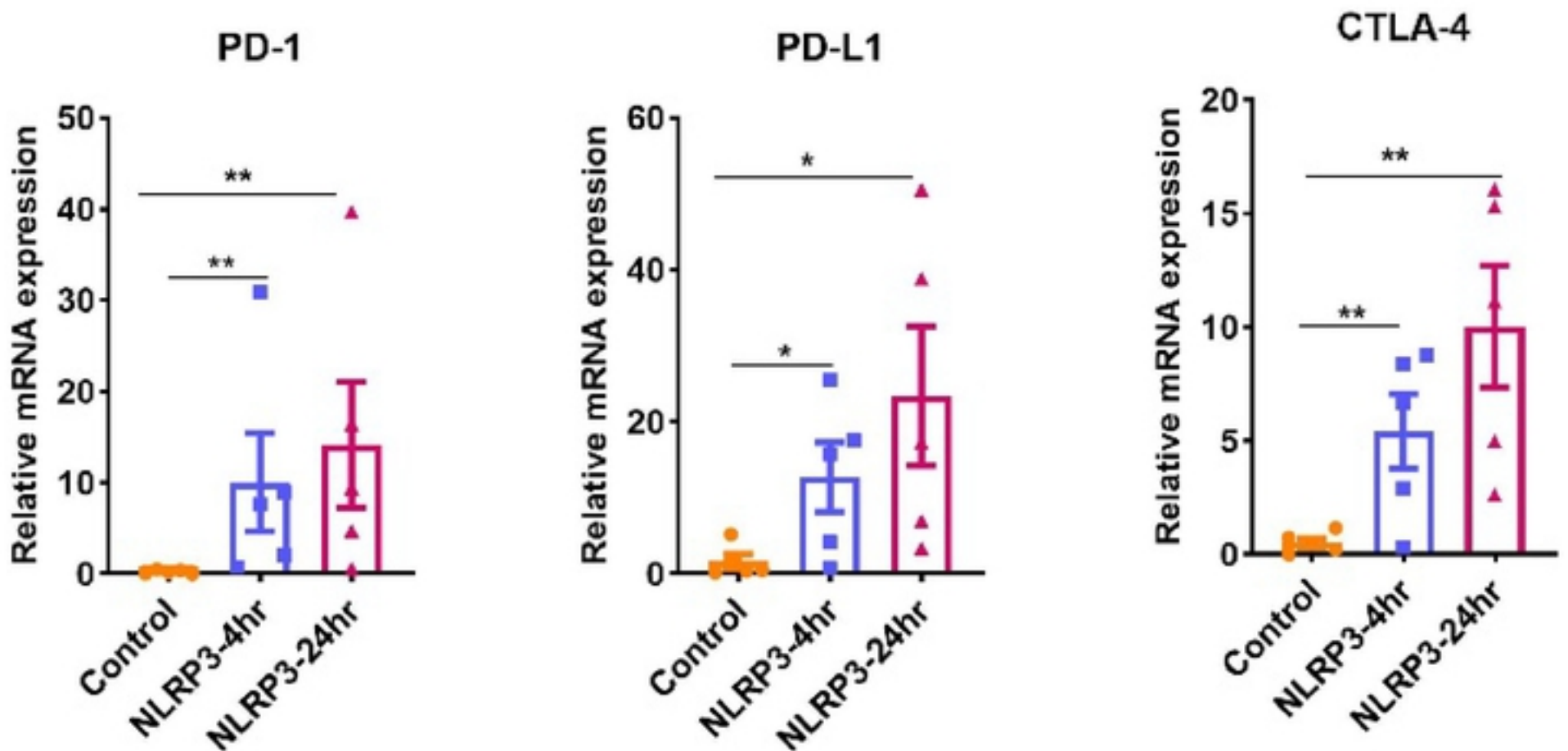
**C**

Figure 4